

C. I. H. Anderson · A. S. Brierley · F. Armstrong

## Spatio-temporal variability in the distribution of epi- and meso-pelagic acoustic backscatter in the Irminger Sea, North Atlantic, with implications for predation on *Calanus finmarchicus*

Received: 11 May 2004 / Accepted: 4 November 2004 / Published online: 17 December 2004  
© Springer-Verlag 2004

**Abstract** The deep scattering layers of the North Atlantic, including the Irminger Sea, contain many predators of the key copepod species *Calanus finmarchicus*. Previous seasonally restricted studies have described the deep acoustic scattering layers of the Irminger Sea as ‘ubiquitous’. They have shown that the intensity of the acoustic backscatter varies across the region, and so, by implication, the potential predation pressure on *C. finmarchicus* also varies spatially. This paper reports observations of the distribution of epipelagic (0–200 m) and meso-pelagic (200–1,000 m) acoustic backscatter in the Irminger Sea, made using a scientific echosounder operating at 38 kHz during four seasonal (winter, spring and summer) cruises. Our study demonstrates that the intensity of the backscatter varies seasonally in regionally distinct ways across the Irminger Sea. The mean acoustic backscatter, both in the upper 800 m and upper 200 m of the water column, varied significantly between the northern, central and southern areas of the central basin (‘open ocean’), and within each area between the Greenland shelf slope, open ocean and Mid-Atlantic Ridge subregions. Different patterns of seasonal change in the acoustic backscatter between the upper 800 m and upper 200 m were also seen, indicating both persistent differences in the underlying amount of backscatter in each area, and varying patterns of seasonal increase in the near surface backscatter in the different areas and subregions. These observations could be related to the different oceanographic regimes encountered in each location, and are discussed in terms

of their implications for potential predation pressure on *C. finmarchicus*.

### Introduction

The Irminger Sea lies in the western sub-Arctic North Atlantic (Fig. 1). It is bounded to the west and north by the continental shelves of Greenland and Iceland, and to the east by the Mid-Atlantic Ridge. The primary current flow is counter-clockwise around its margin (Lavender et al. 2000; Bower et al. 2002). The Irminger Sea can be divided into at least three distinct regions based on the properties of the upper water column (Holliday et al., unpublished data): the region to the west of the crest of the Mid-Atlantic Ridge dominated by the northwards flow of the Irminger Current; the central basin, which contains an oligotrophic, weakly cyclonic gyre; and the region over the Greenland shelf slope dominated by the intense southerly flow of the East Greenland Current (Lavender et al. 2000). The Irminger Current carries relatively warm, saline water derived from the North Atlantic Current, and retroflects at the northern end of the basin to feed the portion of the East Greenland Current that flows over the shelf slope (Holliday et al., unpublished data). This water mass becomes progressively cooler and fresher towards the south as it interacts with colder, fresher water both of polar origin, which flows over the shelf as the inner branch of the East Greenland Current, and from the oceanic waters of the central basin.

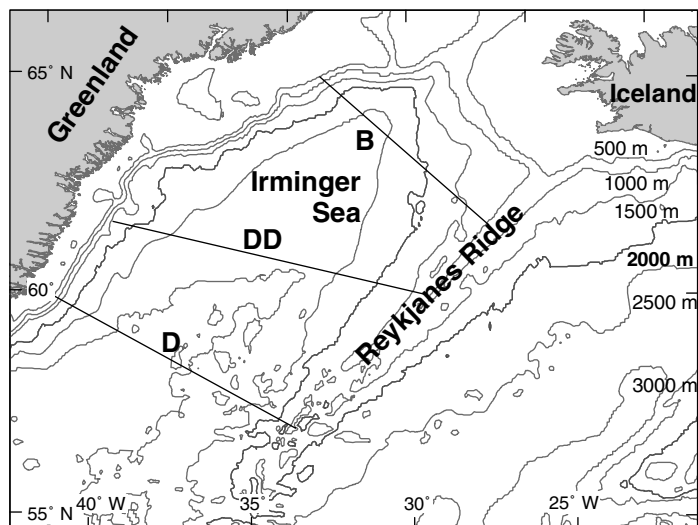
Until recently, most biological research in the Irminger Sea has focussed on the commercially important redfish *Sebastes* spp., for which regular combined acoustic and trawl surveys are conducted (e.g. Sigurdsson et al. 1999). Arising from these studies, it has been observed that meso-pelagic (in the depth zone 200–1,000 m) acoustic deep scattering layers (DSLs) are ‘ubiquitous’ throughout the Irminger Sea and that they show spatial variability in their density (Magnusson

Communicated by J.P. Thorpe, Port Erin

C. I. H. Anderson (✉) · A. S. Brierley  
Gatty Marine Laboratory, University of St Andrews,  
East Sands, St Andrews, KY16 8LB, UK  
E-mail: ciha@st-andrews.ac.uk  
Fax: +0044-1334-463458

F. Armstrong  
FRS Marine Laboratory, 375 Victoria Road,  
PO Box 101, Aberdeen, AB11 9DB, UK

**Fig. 1** The study region with the location of the three transects (*B*, *DD* and *D*) along which data were collected



1996). However, few attempts have been made to quantify this spatial variability, and data have not been available to consider the influence of seasonal variability on the distribution of DSLs in any detail (Sigurdsson et al. 2002). In particular, due to the remote location and the adverse weather conditions that may be experienced, nothing is known about the distribution of the DSLs outside of the spring and summer.

Recent interest in the possible impacts of climate change on global circulation (e.g. Dickson et al. 2002), and the consequences for the ecology of the North Atlantic (e.g. Beaugrand 2003; Greene et al. 2003), have brought attention to bear on the Irminger Sea. This region has the potential to be of major importance for the copepod species *Calanus finmarchicus* (Greene and Pershing 2000), but has not received the attention given to other parts of the North Atlantic (e.g. during the Trans-Atlantic Study of *C. finmarchicus* (TASC) project; Tande and Miller 2000). *C. finmarchicus* is central to the food web of the sub-Arctic North Atlantic, where it performs a key role transferring primary production to higher trophic levels (Parsons and Lalli 1988). Its life-cycle is characterised by an overwintering diapause phase where the animals are found at depths greater than 500 m (Heath et al. 2000). Quantifying mortality during diapause, including that from predation, is considered key to understanding the regional population dynamics of *C. finmarchicus*.

In an effort to expand the geographic extent of observations of *C. finmarchicus*, the Marine Productivity programme, funded by the UK Natural Environment Research Council, was designed to provide a spring, summer and winter examination of *C. finmarchicus* and its environment in the Irminger Sea. As part of this programme, a combination of active acoustic- and net-sampling was used to describe the distribution and abundance of potential predators of *C. finmarchicus* across the region.

Active underway-acoustic sampling, using scientific echosounders, provides a powerful technique for broad-

scale surveys, enabling large areas to be surveyed in short periods of time. It can provide quantitative observations throughout the depth strata where the pelagic biomass is greatest (e.g. up to 1,000 m range at 38 kHz), and the use of a range of frequencies enables both the detection of organisms of different sizes (Holliday and Pieper 1995) and the multi-frequency discrimination of targets (e.g. Brierley et al. 1998). Unlike most net surveys, which produce point data, underway acoustic surveys provide continuous records such that boundaries between different ecological regions can be identified precisely. Acoustic sampling is appropriate for investigating the distribution of a wide range of potential predators of *C. finmarchicus*, as larger predators (e.g. euphausiids and myctophid fish) are major components of the DSLs throughout the North Atlantic including the Irminger Sea region (Magnusson 1996).

This paper reports data from four active acoustic surveys of the Irminger Sea, and provides the first description of seasonal variation in the regional distribution of acoustic backscatter. Backscattering intensity was measured using an echosounder operating at 38 kHz, and so provides a proxy for the distribution of potential macroplanktonic/micronektonic predators of *C. finmarchicus*. The results are considered in light of other aspects of the Marine Productivity programme, and the implications of the potential predation pressure for the population of *C. finmarchicus* in the Irminger Sea are discussed.

## Materials and methods

### Data collection

Acoustic data were collected during four multi-disciplinary research cruises aboard R.R.S. "Discovery" to the Irminger Sea and adjacent waters in the western North Atlantic (Fig. 1). The cruises took place during

early winter 2001 (D258, 1 November–18 December), spring 2002 (D262, 18 April–27 May), summer 2002 (D264, 25 July–28 August) and early winter 2002 (D267, 6 November–18 December). Sampling focussed on three transects running across the basin (approximately southeast–northwest) that were repeated to varying degrees between cruises (Fig. 1). During both winter cruises, and in particular during the second winter (D267), the collection of data was restricted due to the adverse conditions experienced.

Data were collected using a scientific echosounder (Simrad EK500) operating at 38 kHz, 120 kHz and 200 kHz, although only the 38 kHz data are reported here. The echosounder was calibrated at the start of each cruise using standard-target techniques (Foote et al. 1987). The transducers were housed in a towed body, which was deployed at approximately 6 m depth whenever the vessel was underway and conditions allowed. The acoustic data were recorded using Echolog 500 (v. 2.25 SonarData, 1996). Good quality data were collected when the ship was steaming at speeds greater than 7 knots. This paper focuses solely on the 38 kHz data, as this frequency has the greatest range (data collected to 1,000 m depth) and so provides observations overlapping with the upper part of the overwintering depth range of *C. finmarchicus* (generally 500–1,500 m in the open ocean; Heath et al. 2000). Data on the physical properties of the water column (including temperature and salinity) were also collected throughout the cruises using a CTD (see Pollard et al. (2002) for details).

### Data processing

Acoustic data were processed using Echoview analysis software (v. 3.00 SonarData, 2003). They were divided into sets representing continuous periods of usable data, within which areas of bad data (e.g. false bottom echoes) were masked out. The cruise-specific calibration values were applied to each dataset, along with appropriate sound speed and absorption parameters calculated from the depth-weighted average oceanographic conditions experienced during that cruise (see Demer et al. 2004 for method). The echosounder calibrated gain values derived for each cruise suggest that the equipment remained stable throughout the study, with a maximum range in the calculated  $S_v$  gain for the 38 kHz transducer of 0.24 dB (mean  $\pm$  SD 26.67  $\pm$  0.11 dB).

Time-varied gain (TVG)-amplified background noise was removed from each data set following Watkins and Brierley (1996). A second specially developed algorithm was implemented to reduce the impact of stochastic noise spikes that were intermittently apparent in the data, and which were more prevalent with increasing depth down the echograms. The exact cause of the spikes remains unknown, but they appeared related to an interaction of ship-generated noise and sea conditions. To remove the spikes, each sample (1 ping horizontally by 1.43 m vertically) of the calibrated

TVG-noise corrected data was compared in turn to the equivalent sample of the preceding and following pings. Where the ping-to-ping difference was greater than 10 dB (on average in the upper 5% of all difference values) the cell was marked as bad data and was excluded from further analysis. Visual inspection of the echograms before and after spike removal suggested the 10 dB threshold was most appropriate, as it consistently removed a substantial proportion of the noise features whilst preserving the biological features of interest. Without the implementation of the algorithm the lower boundary of the deep scattering layers could not be clearly determined, particularly in data from the winter cruises where the spikes were more prominent. Mean volume backscattering values ( $S_v$ ) from the cleaned data were integrated over 250 m horizontally by 5 m depth. The integrated values were then used to construct sections along each transect, which were used for visual interpretation (e.g. Fig. 2).

### Data analysis

The mean nautical area scattering coefficient (NASC in  $\text{m}^2\text{n mi}^{-2}$ ), a linear measure by square nautical mile of water surface sampled of the total acoustic backscatter per unit volume (MacLennan et al. 2002), was calculated for each 5 km section of cruise track over the full usable depth of the data ('surface' to 800 m) and over the upper 200 m of the water column alone. Data > 800 m depth were excluded from the analyses due to the persistence of unacceptable levels of stochastic noise in many cases, even after the application of the spike removal algorithm. The exclusion of data from the 800–1,000 m depth stratum was justified, given that previous observations of DSLs in the region found them almost exclusively at < 800 m depth (Magnusson 1996).

The integrated data were categorised using the following parameters: cruise (a proxy for season), transect, region along transect, and daylight state (see Table 1 for exact definitions). The region along transect was defined using the 2,000 m isobath as a simple consistent feature that provided an approximation of the boundaries between the three major oceanographic regimes encountered across the basin (Holliday et al., unpublished data). For daylight state, the definition of twilight used (based on the time of nautical twilight; Table 1) was chosen to explicitly encompass the maximum period of the diel vertical migrations seen (e.g. Fig. 2). This means that although some brief periods where the organisms were exhibiting 'day' or 'night' behaviours were included in the twilight category, only genuinely day and night behaviours were included in their respective categories. However, under this definition no night occurred along the northern-most transect (B) during either the spring or summer cruises as the sun never descended far enough below the horizon at that latitude during the period of the cruises.

**Fig. 2** Examples of the sections along each transect of mean volume backscatter ( $S_v$ , dB re  $1 \text{ m}^{-1}$ ): data from the central transect (DD) for the first winter (D258), spring (D262) and summer (D264) cruises. The daylight state in which the data were collected, and the position of the 2,000-m isobath (separating the Greenland slope, open ocean and Mid-Atlantic Ridge regions), are also indicated

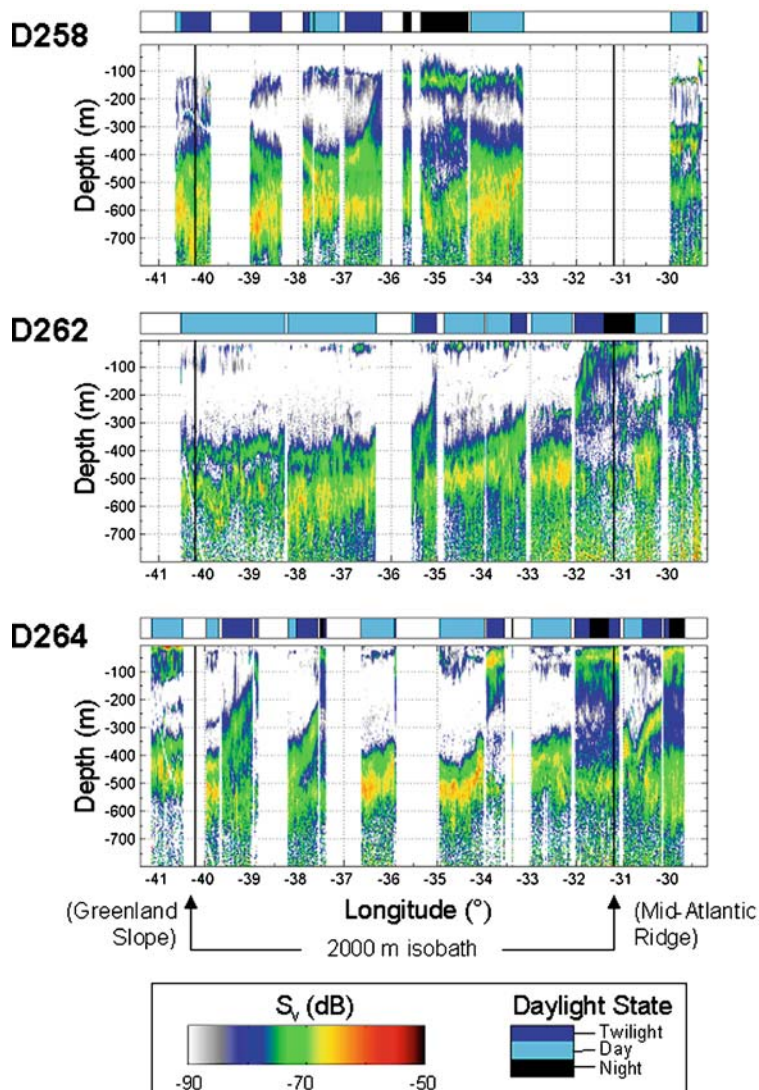


**Table 1** The factors used in classifying the acoustic data, with the definitions of each category used

Factor	Categories			
Cruise	Winter 1D258, November–December 2001	SpringD262, April–May 2002	SummerD264, July–August 2002	Winter 2 D267, November–December 2002
Transect Region (See Fig. 1)	Northernline B Greenland slopewest of 2,000 m isobath	Centralline DD Open ocean > 2,000 m depth	Southernline D Mid-Atlantic Ridge east of 2,000 m isobath to crest of ridge	
Daylight state	Daysunrise + 1 h to sunset	Nightnautical dusk end to nautical dusk start	Twilightsunset to nautical dusk end and nautical dusk start to sunrise + 1 h	

Given that most of the data were not normally distributed, and to allow for the highly variable sampling effort present for each combination of factors, the effects of only one factor were tested at a time and the factors not under examination were kept constant in each analysis. Due to the significant differences in backscatter observed between night and day (see Results), and to the greater availability of data collected during the day,

most statistical tests were carried out on day data only. The twilight data were excluded from all analyses due to the uncertainties caused by the diel vertical migrations occurring during that period. For similar reasons, including the small sample sizes from the Mid-Atlantic Ridge and Greenland slope regions (a function of their limited geographic extent), the tests of the effects of transect and cruise were only carried out on day data



from the open ocean region. To further mitigate the effects of the often small sample sizes, exact significance values were calculated where possible (for the post hoc Mann-Whitney  $U$  tests of the effect of location within transect), and Monte Carlo analyses were used to verify the significance levels of the unadjusted significance values calculated for all other tests (SPSS v11.0 SPSS, 1989–2001).

## Results

### General description

Our observations are consistent with reports from previous, seasonally restricted, surveys that suggested that deep scattering layers (DSLs) were ubiquitous in the Irminger Sea. Inspection of the individual echograms and along-transect sections showed that layers ( $S_v$  threshold  $-80$  dB) extended across all parts of the region, regardless of location or season, wherever the water depth was greater than 500 m (e.g. Fig. 2).

The basic structuring of both the epi- and meso-pelagic (deep) scattering layers was also consistent. A distinct, and generally single, layer (typically 20–80 m in vertical extent) was found in the upper 200 m of the water column. This epi-pelagic upper layer occurred between 100 m and 200 m depth in winter, in both D258 and D267, and between the surface and 100 m depth in spring (D262) and in summer (D264, e.g. Fig. 2). During the spring/summer period, the layer was found predominantly in the upper 50 m of the water column and frequently extended to the surface. The top of the upper layer generally only coincided with the surface at night, but this behaviour was observed during both day and night in the Greenland slope region during the summer cruise (e.g. Fig. 2).

In the Mid-Atlantic Ridge region of each transect, an additional upper layer was frequently seen in the top 200 m, and was particularly distinct along the central transect (DD). Whilst the main upper layer generally consisted of a diffuse band of relatively low intensity backscatter with higher intensity areas embedded in it (in the order of 5–10 dB difference), the feature confined to the Mid-Atlantic Ridge region was made up of small discrete higher intensity structures arranged into a horizontal layer.

Below 300 m depth a more complex region of DSLs was consistently seen. This depth stratum normally contained at least two bands of higher intensity backscatter, which generally formed distinct layers or structures within a more diffuse broad layer. The vertical extent of the broad layer was generally 250–400 m, with a difference in intensity between the weaker and stronger components in the order of 5 dB. Along the northern transect (B), a third distinct intermediate layer (50–80 m vertical extent) was seen consistently in the 200–300 m depth stratum between the upper layer and the band of deep layers, which were still only found below 300 m.

Obvious diel vertical migrations were seen consistently between the deep and upper layers, with an upwards movement of part of the deep layer after sunset, followed by a return near dawn (e.g. Fig. 2). During the winter, this upward migration did not appear to proceed beyond the main upper layer, even though this layer was located at greater than 100 m depth. During the spring and summer, the upward migration was accompanied by a decrease in the minimum depth of the upper layer, which sometimes included the layer extending to the surface.

For the southern-most transect (D), which was only surveyed during the summer (cruise D264), the upper layer in the middle of the basin was predominantly found below 50 m depth during the day. It appeared more similar in form to that seen during the winter than during the summer along the central transect (DD). However, the lack of data collected during the night along the southern-most transect prevented the determination of the upper extent of the diel vertical migration.

Maps of the distribution of mean NASC to 800 m (Fig. 3) and to 200 m (Fig. 4) show regional, diel and seasonal differences in the distribution of 38 kHz backscatter, and reveal that the variation in the backscatter in the upper layer is different to that of the backscatter of the water column as a whole at any given location. Two features are particularly striking in the maps of mean NASC to 200 m (Fig. 4). Firstly, the extremely low levels of backscatter along the central transect (DD) compared to the northern (B) and southern (D) transects during the spring and summer cruises (D262 and D264). Secondly, the seasonal increase in backscatter between the spring and summer cruises in the Mid-Atlantic Ridge region at the end of the northern transect (B) and along the Greenland slope for the central and southern transects (DD and D).

### Day versus night

Analysis of overall mean NASC from the surface (i.e. depth of the transducer) to 800 m for all combinations of cruise-transect-region where both day and night data were available (Table 2a) showed there was significantly less detectable backscatter at night than during the day (Paired  $t$ -test, all observations,  $t=2.657$ ,  $df=7$ ,  $P=0.033$ ). The day–night difference was also significant for the open ocean values considered alone (Paired  $t$ -test  $t=3.663$ ,  $df=3$ ,  $P=0.035$ ), but not for the Mid-Atlantic Ridge values where a single high nighttime observation (transect DD cruise D264) reversed the trend. When the same test was applied to the mean NASC in the upper 200 m of the water column (the location of the upper layer, Table 2b) the opposite pattern was seen, with significantly higher backscatter detected at night than during the day (Paired  $t$ -test, all observations,  $t=-3.440$ ,  $df=7$ ,  $P=0.011$ ). This reversed pattern was consistent across all observations, but was only mar-

**Fig. 3** Mean nautical area scattering coefficient (*NASC*,  $m^2 n mi^{-2}$ ) integrated over the top 800 m of the water column (for each 5-km section of cruise track) from the first winter (*D258*), spring (*D262*) and summer (*D264*) cruises. Only data collected during the day are shown, and no data from the second winter cruise are given as very little was collected

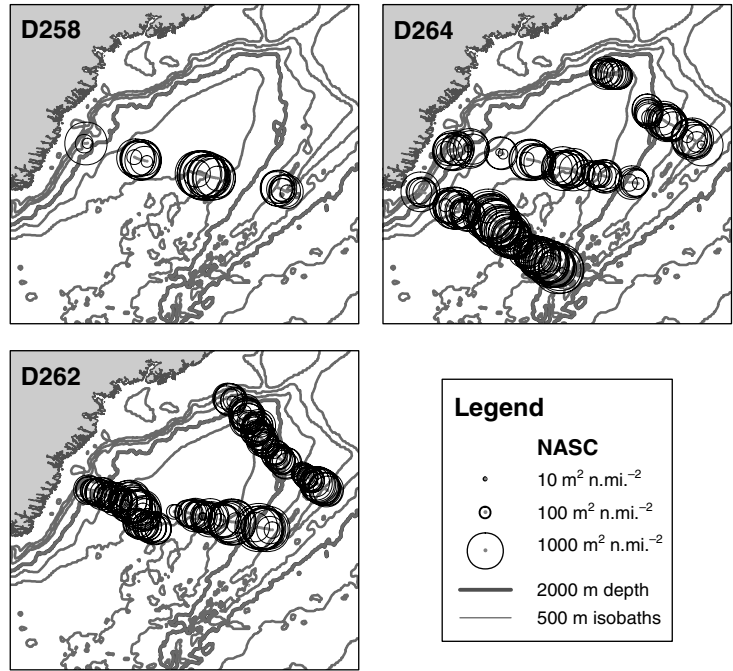
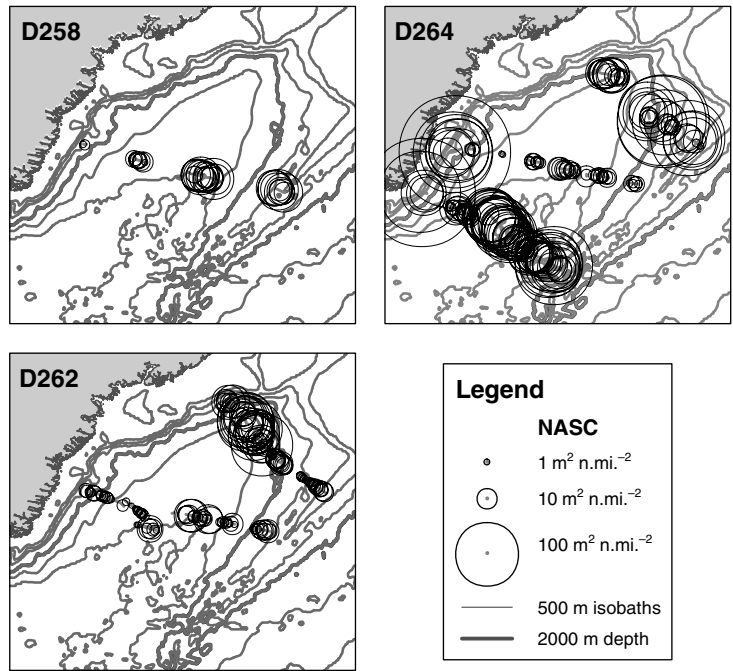


**Fig. 4** Mean *NASC* ( $m^2 n mi^{-2}$ ) integrated over the top 200 m of the water column (for each 5-km section of cruise track) from the first winter (*D258*), spring (*D262*) and summer (*D264*) cruises. Only data collected during the day are shown, and no data from the second winter cruise are given as very little was collected



ginally significant when the values from each region were considered separately (Paired *t*-tests: open ocean  $t = -2.576$ ,  $df = 3$ ,  $P = 0.082$ ; Mid-Atlantic Ridge  $t = -3.148$ ,  $df = 3$ ,  $P = 0.051$ ).

Effects of transect within each cruise (season)

For the data from the open ocean region collected within a single cruise, significant differences were found in the mean *NASC* in the upper 800 m of the water column

between each transect (Fig. 3, Table 2a). For the spring cruise (*D262*), the mean *NASC* was significantly lower along the northern-most (B) transect than the central (DD) transect (Mann-Whitney *U* test:  $U = 1644.0$ ,  $P = 0.013$ ). For the summer cruise (*D264*), significant differences in the mean *NASC* were found between the northern (B), central (DD) and southern (D) transects (Kruskal-Wallis test:  $\chi^2 = 29.886$ ,  $df = 2$ ,  $P < 0.001$ ). Post hoc Mann-Whitney *U* tests found significant differences between each pair of transects (Mann-Whitney *U*: B vs DD  $U = 209.0$   $P = 0.011$ , DD vs D  $U = 936.0$ ,  $P < 0.001$ ,

**Table 2** Mean nautical area scattering coefficient (NASC) values ( $\text{m}^2\text{n mi}^{-2}$ ) for available day and night data integrated within transect, cruise and region along transect for *A* the upper 800 m

and *B* the upper 200 m of the water column. The minimum and maximum individual mean NASC values integrated over 5-km sections of cruise track and the same depth ranges are also given

Transect	Cruise	Region along transect			
		Open ocean		Mid-Atlantic Ridge	
		Day	Night	Day	Night
<b>A</b>					
Central (DD)	Winter 1 (D258)	1844.9 (153.5–2963.3)	1107.8 (173.6–1919.3)	1858.2 (313.2 - 2885.2)	–
	Spring (D262)	1117.6 (53.9–2677.2)	531.4 (121.1–942.2)	1858.2 (313.2 - 2885.2)	565.7 (224.7–862.3)
	Summer (D264)	1222.2 (69.9–2352.4)	825.6 (118.3–1298.6)	792.7 (162.0–1354.1)	1257.2 (41.3–2147.6)
	Winter 2 (D267)	–	–	597.2 (372.8–909.4)	366.0 (264.8–458.6)
Southern (D)	Summer (D264)	1688.4 (55.2–3228.5)	319.3 (74.7–595.7)	1978.3 (44.5–3096.9)	1664.3 (701.5–2082.8)
<b>B</b>					
Central (DD)	Winter 1 (D258)	24.9 (1.4–69.7)	74.1 (8.1–136.2)	–	–
	Spring (D262)	5.3 (0.1–43.4)	42.0 (9.8–62.1)	9.4 (1.6–21.3)	66.6 (29.6–89.6)
	Summer (D264)	7.7 (0.2–21.5)	96.0 (11.4–186.3)	5.9 (1.9–10.4)	146.2 (5.5–288.9)
	Winter 2 (D267)	–	–	33.2 (17.0–51.0)	93.9 (62.1–150.9)
Southern (D)	Summer (D264)	61.9 (0.7–248.7)	66.3 (24.6–114.9)	20.4 (0.6–33.5)	235.8 (98.6–378.5)

**B** vs **D**  $U=213.0$   $P < 0.001$ ), with the southern (**D**) transect showing the highest mean NASC value followed by the central (**DD**) and then northern (**B**) transects.

For the tests of mean NASC in the upper 200 m of the water column (Fig. 4, Table 2b), the same patterns of significance were found as for the 0- to 800-m analysis, but the trends underlying them were slightly different. In contrast to the results for mean NASC in the upper 800 m, during the spring cruise (D262) the mean NASC in the upper 200 m was significantly higher along the northern-most (**B**) transect than on the central (**DD**) transect (Mann-Whitney  $U$  test:  $U=792.0$   $P < 0.001$ ). The comparison between the three transects for the summer cruise (D262) was again significant both overall (Kruskal-Wallis test:  $\chi^2=50.110$   $df=2$   $P < 0.001$ ) and between each pair of transects (Mann-Whitney  $U$ : **B** vs **DD**  $U=91.0$ ,  $P < 0.001$ ; **DD** vs **D**  $U=392.0$ ,  $P < 0.001$ ; **B** vs **D**  $U=502.0$ ,  $P=0.045$ ), with the highest overall mean NASC value seen for the southern-most transect (**D**). However, the rank position of the northern (**B**) and central (**DD**) transects was reversed, with the northern transect showing the higher overall mean NASC.

#### Effects of cruise (season) within each transect

For the data from the open ocean region collected from a single transect, significant differences were found in the mean NASC in the upper 800 m of the water column between some, but not all, cruises (Table 2a). For the northern-most (**B**) transect, no significant difference in the mean NASC was found between the spring cruise (D262) and summer cruise (D264) (Mann-Whitney  $U$  test). For the central transect (**DD**), significant differences in the mean NASC were found between the first winter (D258), spring (D262) and summer (D264) cruises (Kruskal-Wallis test:  $\chi^2=18.631$ ,  $df=2$ ,  $P < 0.001$ ). Post hoc Mann-Whitney  $U$  tests revealed significant differences between the winter cruise and each of the

spring and summer cruises, but not between the spring and summer cruises themselves (Mann-Whitney  $U$ : D258 vs D262  $U=467.0$ ,  $P < 0.001$ ; D258 vs D264  $U=226.0$ ,  $P=0.001$ ). The first winter cruise (D258) showed a higher overall mean NASC values than either the spring (D262) or summer (D264) cruises.

For the tests of mean NASC in the upper 200 m of the water column (Table 2b), subtly different patterns of significance were found. As with the 800-m data, no significant differences were found between the spring cruise (D262) and summer cruise (D264) along the northern (**B**) transect (Mann-Whitney  $U$  test). For the central transect (**DD**), significant differences in the mean NASC were again found between the first winter (D258), spring (D262) and summer (D264) cruises (Kruskal-Wallis test:  $\chi^2=43.554$ ,  $df=2$ ,  $P < 0.001$ ). However, the post hoc Mann-Whitney  $U$  tests revealed significant differences between all three combinations of cruises (Mann-Whitney  $U$ : D258 vs D262  $U=233.0$ ,  $P < 0.001$ ; D258 vs D264  $U=158.0$ ,  $P < 0.001$ ; D262 vs D264  $U=1037.0$ ,  $P < 0.001$ ). The highest mean NASC value was found for the first winter cruise (D258), followed by the summer (D264), and then spring (D262) cruises.

#### Region along transect

The effects of region along a transect were investigated using Kruskal-Wallis tests on the mean NASC to 800 m depth (Fig. 3) and to 200 m depth (Fig. 4) for all the available combinations of cruise and transect with daytime data from all three regions (see Table 3 for values and Table 4 for test results). Post hoc Mann-Whitney  $U$  tests were used to further investigate the significant results of the initial tests (Table 5). In all instances where significant differences were detected, it was the values from the Mid-Atlantic Ridge region that appeared to drive these differences (Table 5). For the tests of NASC to 800 m depth where a significant

**Table 3** Mean NASC values (m<sup>2</sup>n mi<sup>-2</sup>) for available day data integrated within cruise, transect and region along transect for A the upper 800 m and B the upper 200 m of the water column. The

minimum and maximum individual mean NASC values integrated over 5 km sections of cruise track and the same depth ranges are also given

Cruise	Transect	Region along transect		
		Greenland slope	Open ocean	Mid-Atlantic Ridge
<b>A</b>				
Winter 1 (D258)	Central (DD)	938.3 (119.6–2292.9)	1844.9 (153.5–2963.3)	1081.9 (246.8–1626.1)
Spring (D262)	Northern (B)	847.7 (138.5–1288.4)	911.8 (241.8–1711.7)	952.2 (75.7–1556.6)
	Central (DD)	811.0 (607.8–1035.6)	1117.6 (53.9–2677.2)	1858.2 (313.2–2885.2)
Summer (D264)	Northern (B)	678.9 (325.7–1005.7)	939.2 (307.2–1292.6)	1281.7 (83.4–2219.7)
	Central (DD)	1243.3 (497.5–2015.6)	1222.2 (69.9–2352.4)	792.7 (162.0–1354.1)
	Southern (D)	1126.7 (756.2–1935.6)	1688.4 (55.2–3228.5)	1978.3 (44.5–3096.9)
<b>B</b>				
Winter 1 (D258)	Central (DD)	2.9 (1.9–3.9)	24.9 (1.4–69.7)	40.7 (17.4–67.4)
Spring (D262)	Northern (B)	21.8 (7.4–47.0)	38.2 (0.2–157.8)	5.8 (0.4–14.7)
	Central (DD)	4.9 (1.2–7.9)	5.3 (0.1–43.4)	9.4 (1.6–21.3)
Summer (D264)	Northern (B)	34.7 (24.6–41.4)	36.8 (6.8–142.2)	91.6 (1.8–349.9)
	Central (DD)	178.3 (36.3–515.0)	7.7 (0.16–21.5)	5.9 (1.9–10.4)
	Southern (D)	187.4 (44.2–481.3)	61.9 (0.68–248.7)	20.4 (0.58–33.5)

**Table 4** Summary of the results of the Kruskal-Wallis tests of mean NASC by region (Greenland slope, open ocean and Mid-Atlantic Ridge) within each available transect-cruise combination.

Mean NASC was calculated for both the upper 800 m and upper 200 m of the water column using day data only ( $-P > 0.10$ , \*  $0.05 < P < 0.10$ , \*\*  $0.01 < P < 0.05$ , \*\*\*  $P < 0.01$ )

	Mean NASC to 800 m depth			Mean NASC to 200 m depth		
	Winter 1 (D258)	Spring (D262)	Summer (D264)	Winter 1 (D258)	Spring (D262)	Summer (D264)
Northern (B)		–	***		***	–
Central (DD)	**	***	–	**	***	***
Southern (D)			*			**

**Test results to 800 m depth** B D262  $\chi^2 = 0.157, df = 2, P = 0.924$  B D264  $\chi^2 = 10.592, df = 2, P = 0.005$  DD D258  $\chi^2 = 8.122, df = 2, P = 0.017$  DD D262  $\chi^2 = 11.271, df = 2, P = 0.004$  DD D264  $\chi^2 = 3.571, df = 2, P = 0.168$  D D264  $\chi^2 = 4.914, df = 2, P = 0.086$  **Test**

**results to 200 m depth** B D262  $\chi^2 = 18.834, df = 2, P < 0.001$  B D264  $\chi^2 = 1.462, df = 2, P = 0.481$  DD D258  $\chi^2 = 9.109, df = 2, P = 0.011$  DD D262  $\chi^2 = 10.272, df = 2, P = 0.006$  DD D264  $\chi^2 = 22.609, df = 2, P < 0.001$  D D264  $\chi^2 = 6.420, df = 2, P = 0.040$

**Table 5** Summary of the significant results of the post-hoc Mann-Whitney U tests of A mean NASC to 800 m and B mean NASC to 200 m, used to further investigate the significant results of the Kruskal-Wallis tests exploring the effects of region within cruise-

transect shown in Table 4. Exact probabilities are given where calculated (OO = open ocean, GS = Greenland slope, M-AR = Mid-Atlantic Ridge; \*\*  $0.01 < P < 0.05$ , \*\*\*  $P < 0.01$ )

	Winter 1 (D258)	Spring (D262)	Summer (D264)
<b>A<sup>a</sup></b>			
Northern (B)			OO < M-AR ***
Central (DD)	OO > M-AR ***	GS < M-AR **, OO < M-AR ***	
Southern (D)			
<b>B<sup>b</sup></b>			
Northern (B)		GS < M-AR ***, OO < M-AR ***	
Central (DD)	GS < OO **, GS < M-AR **, OO < M-AR **	OO < M-AR ***	GS > OO ***, GS > M-AR ***
Southern (D)			GS < M-AR **

<sup>a</sup> Significant test results: B D264 OO vs M-AR U = 83.00, Exact  $P = 0.004$  DD D258 OO vs M-AR U = 38.00, Exact  $P = 0.005$  DD D262 GS vs M-AR U = 5.00, Exact  $P = 0.026$ ; OO vs M-AR U = 219.00, Exact  $P = 0.003$  <sup>b</sup> Significant test results: B D262 GS vs M-AR U = 9.00, Exact  $P = 0.001$ ; OO vs M-AR U = 294.00, Exact

$P < 0.001$  DD D258 GS vs OO U = 3.00, Exact  $P = 0.040$ ; GS vs M-AR U = 0.00, Exact  $P = 0.036$ ; OO v M-AR U = 50.00, Exact  $P = 0.024$  DD D262 OO vs M-AR U = 215.00, Exact  $P = 0.002$  DD D264 GS vs OO U = 0.00, Exact  $P < 0.001$ ; GS vs M-AR U = 0.00, Exact  $P < 0.001$  D D264 GS vs M-AR U = 0.0,0 Exact  $P = 0.016$

difference was found between the regions, the Mid-Atlantic Ridge values were significantly higher than either the Greenland slope or the open ocean values during both the spring (D262, along the central transect) and summer (D264, along the northern transect)

cruises. During the winter cruise, the Mid-Atlantic Ridge values were significantly lower than the open ocean values along the central transect (DD).

For the tests of NASC to 200 m depth where a significant difference was found between the regions,



the results are slightly more complex. The Mid-Atlantic Ridge values were significantly higher than either the Greenland slope or the open ocean values during both the winter (D258, along the central transect) and spring (D262, along the central and northern transects) cruises. The open ocean values were also significantly higher than the Greenland slope values during the winter cruise (D258, along the central transect). However, during the summer cruise (D264), the Greenland slope values were significantly higher than both the open ocean and Mid-Atlantic Ridge values along the central transect (DD). The order was reversed along the southern transect (D), where the Mid-Atlantic Ridge values were again significantly higher than the Greenland slope values.

---

## Discussion

This study was undertaken to provide insight into possible spatial and seasonal variation in the potential predation pressure on *C. finmarchicus* from macrozooplankton and micronekton. As only a single frequency (38 kHz) of echosounder data was used, and no net data were incorporated into the analysis, it was not possible to partition the observed backscatter into classes of backscattering organisms. However, the concentration of known predators of *C. finmarchicus*, including myctophid fish (Sameoto 1989) and euphausiids (Båmstedt and Karlson 1998), in the deep scattering layers across the North Atlantic including the Irminger Sea has previously been demonstrated (Magnusson 1996), and their presence confirmed through the use of net sampling during the Marine Productivity cruises (R. Saunders, personal communication). Therefore, the backscatter at 38 kHz, and in particular the location of the acoustic scattering layers, provides a useful proxy for understanding the broadscale distribution of potential predators of *C. finmarchicus*, and this approach has been used in previous, less comprehensive, studies of other parts of the Atlantic (e.g. Dale et al. 1999). Future multi-frequency analysis of data from the upper water column (depth restricted by the limited penetration of higher frequencies), and incorporation of species composition data from net samples, will provide a more detailed analysis of the distribution of specific predators. It will then be possible to make distinctions between increases or differences in backscatter due to the relative abundance of low biomass organisms such as shelled pteropods which are not significant predators of *C. finmarchicus*, and those due to the relative abundance of more significant species to this analysis such as euphausiids.

The results of this study are in agreement with the limited observations of Magnusson (1996), and are broadly similar to the brief description given by Sigurdsson et al. (2002), which provide the only previously published descriptions of the acoustic backscatter in the region. As it is not clear to what depth the backscatter

was integrated in these previous studies, and given that Sigurdsson et al. (2002) show only 'non-redfish' backscatter, exact comparisons are not possible. However, the results presented here do enable a quantification of some of the patterns previously suggested by these authors, such as regional variability in the intensity of the backscatter and the possibility of some degree of seasonal variability.

In the analysis of day versus night data for NASC to 800 m depth, it would be expected that during the night either more backscatter would be detected due to animals migrating upwards into the vertical range of the transducers, or approximately the same amount of backscatter would be detected if the whole of the migrating biomass was already within range (i.e. above 800 m depth) during the day. However, significantly less backscatter was detected at night in most cases, in contrast to the analysis of NASC to 200 m depth where the expected night-time increase was observed. This reduction in observed backscatter to 800 m at night may be due to a combination of factors. A substantial proportion of the backscattering biomass may have migrated above the depth of the transducers (approximately 6 m) and so been lost from the analysis. Alternatively, changes in the behaviour of the animals may have significantly decreased their individual target strengths and so reduced the overall backscatter detected. Both of these factors have been found to apply in acoustic surveys of Antarctic krill *Euphausia superba*. In one study, a 49.5% average underestimation of biomass present was attributed to migration above the depth of the transducers at night (Demer and Hewitt 1995). In another, it was noted that a 10° change in the tilt angle of an animal, possibly caused by diving to avoid a survey vessel in close proximity, could produce a 13.8 dB reduction in individual target strength (Brierley et al. 2003 citing McGehee et al. 1998). A third factor that should be considered is the effects of the reduction in pressure with decreasing depth on individual target strength due to changes in shape and/or relative density of gas-filled organs such as swim bladders or gas vesicles (e.g. Gorska and Ona 2003).

Even given the factors considered above, the lack of an increase in mean NASC to 800 m at night, or even maintenance of the same value as during the day, suggests it is unlikely that a substantial amount of backscattering biomass is migrating up into the range of the transducers at night (except possibly in the Mid-Atlantic Ridge region). This confirms the initial impression from visual inspection of the echograms that the deep scattering layers are nearly always found at less than 800 m depth, as suggested by Magnusson (1996), and definitely above 1,000 m depth. Inspection of echograms from an equivalent lowered echosounder system deployed to 500 m depth at a number of stations during the cruise programme (unpublished data) confirmed that no further acoustic scattering layers existed, in the range of 500 to 1,500 m depth, below those seen from the surface.

This has significant implications for the predation pressure on *C. finmarchicus* during the winter when the majority of its population is found between approximately 500 m and 2,000 m depth in the northern Irminger Basin (Heath et al. 2004). That the overlap with the deep scattering layers is limited suggests that a large proportion of the *C. finmarchicus* population is in a depth refuge from the intense predation likely to be found in the scattering layers, and that the majority of CVI stage females, which are found below approximately 800 m depth, may be almost entirely free of this predation pressure during the winter. These observations provide partial support to the hypothesis that avoidance of planktivorous predators is a primary evolutionary pressure in the selection of different depth habitats by overwintering *C. finmarchicus* in different regions (Dale et al. 1999). However, the incomplete depth separation of the acoustic scattering layers and the region containing a high density of copepods suggest that other factors are also important. Irigoien (2004) suggests that a suite of factors may determine overwintering depth in *C. finmarchicus*. These include requirements both to be below the convective mixed layer depth at the onset of winter, and for females to contain adequate lipid reserves (which control the depth of neutral buoyancy in any given water mass) to allow production of eggs before the onset of the spring bloom. The preferred winter depth of the organisms that make up the DSLs will also be influenced by further factors than simply the availability of *C. finmarchicus*.

Inspection of the echograms suggested that there was almost no backscatter near the surface during the winter cruises, implying an absence of concentrations of predators of *C. finmarchicus* in the upper 50 m of the water column. This has implications for the predation on *C. finmarchicus* when they ascend at the end of diapause. It has been established that although coincidence with the spring phytoplankton bloom is not necessary for egg production in this species, it is required for recruitment of nauplii to the copepodite stages (Irigoien et al. 2003). This may lead to evolutionary pressure on *C. finmarchicus* to conserve resources by remaining in diapause until later in the season. However, if near-surface predation can be avoided by an earlier ascent this may produce an opposing evolutionary pressure leading to the range of ascent times seen. A similar mechanism, based on the avoidance of the spring arrival of migratory fish by the early termination of diapause, has been proposed for *C. finmarchicus* in the Norwegian Sea (Kaartvedt 2000).

For the analyses of mean NASC to 800 m and to 200 m the effects of cruise (season) and transect are subtly different. The results from the analyses of mean NASC to 800 m primarily indicate persistent intrinsic differences in the underlying amount of backscatter, and therefore likely biomass, in the open ocean regions of the north, central and southern basin (as suggested by Magnusson 1996), whilst the results from the analyses of mean NASC to 200 m appear to indicate a spatially

variable seasonal build-up of near-surface biomass overlaid on these intrinsic differences. No comparison of the seasonal differences is possible with the previous authors as the data they present are too seasonally limited.

The effects of region within each transect on the observed backscatter are complex, and again vary between the mean NASC to 800 m and that to 200 m. The significant relationships found in the mean NASC to 800 m depth appear to be driven by the amount of backscatter in the Mid-Atlantic Ridge region. In the winter this is significantly lower than the adjacent open ocean backscatter (DD line), whilst in spring (DD line) and summer (D line) it is significantly higher. This observation is in agreement with the high non-redfish acoustic backscatter found to the west of the Mid-Atlantic Ridge by Sigurdsson et al. (2002) during summer and attributed to the deep-scattering layers. Overall, these observations suggest that while there is little seasonal difference in the underlying amount of backscatter in the open ocean regions of each section of the basin, the Mid-Atlantic Ridge regions show both seasonal and spatial variability.

The results of the analysis of the effects of region on the mean NASC to 200 m show a slightly different pattern, with both the Mid-Atlantic Ridge and Greenland slope regions influencing the results. On the central transect (DD), there is a transition from the Mid-Atlantic Ridge region having the highest backscatter in the winter, to it having equivalent backscatter to the Greenland slope in the spring (still significantly higher than the open ocean region), to the Greenland slope region having the highest backscatter of all three regions in the summer. This implies a spatially variable seasonal build-up in near-surface biomass. The high winter values in the Mid-Atlantic Ridge region may be partially explained by the presence of an extra layer in the upper 200 m of the water column in this area, whilst the spring and summer relationships appear to be driven by the accumulation of biomass over the Greenland shelf slope.

These observations can be related to the biophysical zones found across the region. Three major oceanographic regimes have been defined for the upper 500 m of the water column: the central Irminger Basin; the northward flowing Irminger Current to the west of the Mid-Atlantic Ridge; and the outer portion of the East Greenland Current flowing south over the Greenland shelf slope (Holliday et al., unpublished data). Both the Irminger and East Greenland Currents are further subdivided into northern and southern sections. The central Irminger Basin corresponds to the open ocean region, and is typified by relatively low summer levels of chlorophyll-a ( $0.5 \text{ mg m}^{-3}$ ) in the upper 50 m, which may explain the low levels of near-surface backscatter seen in this region in spring and summer. The southern Irminger Current corresponds approximately to the Mid-Atlantic Ridge regions of the central (DD) and southern (D) transects, whilst the northern Irminger Current flows

along the line of the northern transect (B). The latter region is typified by much higher levels of chlorophyll-a (up to  $2.0 \text{ mg m}^{-3}$ ) in spring than the more southerly portions of the current, and this is reflected both in the near surface and 'full-depth' backscatter observed. The East Greenland Current water considered here primarily originates in the northern Irminger Current, but shows only moderate levels of chlorophyll-a in spring and summer. Finally, distinct Reykjanes Ridge mode water was found at the eastern ends of the central and northern transects approximately within the 1,500 m isobath. This may be associated with the distinctive extra upper backscattering layer (comprised of small discrete high intensity structures) seen at the eastern end of these transects.

Two further investigations carried out as part of the Marine Productivity programme provide supplementary data in support of the interpretation of the acoustic results made here. Analysis of nutrient draw down and calculations of new production values in the northern and central basin found that higher levels of nitrate draw down, associated with increased export production, are found on the Greenland Shelf, along the northern transect and at the eastern (Mid-Atlantic Ridge) end of the central transect (Sanders et al. 2004). The authors suggest that production begins at the margins of the gyre, reflecting the patterns of the increase in backscattering biomass in the upper levels of water column detected in the acoustic data.

Length frequency analysis of three common euphausiid species collected at stations across the study region suggests that population-dynamic processes vary spatially (R. Saunders, personal communication). Preliminary results indicate that populations reach a more advanced state earlier in the year in the northern basin (equivalent to transect B) as opposed to the central basin (transect DD). This is in agreement with the idea that the populations of organisms that constitute the backscattering biomass are increasing first in the northern part of the basin.

Overall, it can be seen that while the deep acoustic scattering layers of the Irminger Sea are ubiquitous (Magnusson 1996), the distribution of acoustic backscatter throughout the water column shows a complex pattern of seasonal and spatial variability. This has significant implications for the potential predation pressure on *C. finmarchicus* across the region. Any more detailed studies of aspects of the acoustic characteristics of the region, including investigations of the distribution and abundance of specific organisms, must account for this underlying variability.

**Acknowledgements** This work was funded by the Natural Environment Research Council, UK under the Marine Productivity Thematic Programme. We wish to thank J. Hunter and all the members of the Fishery Independent Methods Group, FRS Marine Laboratory, Aberdeen for providing both equipment and invaluable technical support; and the Masters, officers and crew of *RRS Discovery*, along with the members of the scientific parties of each Marine Productivity cruise, for all their assistance at sea.

## References

- Båmstedt U, Karlson K (1998) Euphausiid predation on copepods in coastal waters of the Northeast Atlantic. *Mar Ecol Prog Ser* 172:149–168
- Beaugrand G (2003) Long-term changes in copepod abundance and diversity in the north-east Atlantic in relation to fluctuations in the hydroclimatic environment. *Fish Ocean* 12:270–283
- Bower AS, Le Cann B, Rossby T, Zenk W, Gould J, Speer K, Richardson PL, Prater MD, Zhang H-M (2002) Directly measured mid-depth circulation in the northeastern Atlantic. *Nature* 419:603–607
- Brierley AS, Ward P, Watkins JL, Goss C (1998) Acoustic discrimination of Southern Ocean zooplankton. *Deep-Sea Res II* 45:1155–1173
- Brierley AS, Fernandes PG, Brandon MA, Armstrong F, Millard NW, McPhail SD, Stevenson P, Pebody M, Perret J, Squires M, Bone DG, Griffiths G (2003) An investigation of avoidance by Antarctic krill of RRS *James Clark Ross* using the *Autosub-2* autonomous underwater vehicle. *Fish Res* 60:569–576
- Dale T, Bagoien E, Webjørn M, Kaartvedt S (1999) Can predator avoidance explain varying overwintering depth of *Calanus* in different oceanic water masses? *Mar Ecol Prog Ser* 179:113–121
- Demer DA (2004) An estimate of error for the CCAMLR 2000 survey estimate of krill biomass. *Deep-Sea Res II* 51:1237–1251
- Demer DA, Hewitt RP (1995) Bias in acoustic biomass estimates of *Euphausia superba* due to diel vertical migration. *Deep-Sea Res I* 42:455–475
- Dickson B, Yashayaev I, Meincke J, Turrell B, Dye S, Holfort J (2002) Rapid freshening of the deep North Atlantic Ocean over the past four decades. *Nature* 416:832–837
- Foote KG, Knudsen HP, Vestnes G, MacLennan DN, Simmonds E (1987) Calibration of acoustic instruments for fish density estimation: a practical guide. ICES Cooperative Research Report 144, International Council for the Exploration of the Sea, Copenhagen
- Gorska N, Ona E (2003) Modelling the acoustic effect of swim-bladder compression on the acoustic backscattering from herring at normal or near-normal dorsal incidences. *ICES J Mar Sci* 60:1381–1391
- Greene CH, Pershing AJ (2000) The response of *Calanus finmarchicus* populations to climate variability in the Northwest Atlantic: basin-scale forcing associated with the North Atlantic Oscillation. *ICES J Mar Sci* 57:1536–1544
- Greene CH, Pershing AJ, Conversi A, Planque B, Hannah C, Sameoto D, Head E, Smith PC, Reid PC, Jossi J, Mountain D, Benfield MC, Wiebe PH, Durbin E (2003) Trans-Atlantic responses of *Calanus finmarchicus* populations to basin-scale forcing associated with the North Atlantic Oscillation. *Prog Oceanogr* 58:301–312
- Heath MR, Fraser JG, Gislason A, Hay SJ, Jonasdottir SH, Richardson K (2000) Winter distribution of *Calanus finmarchicus* in the Northeast Atlantic. *ICES J Mar Sci* 57:1628–1635
- Heath MR, Boyle PR, Gislason A, Gurney WSC, Hay SJ, Head EJH, Holmes S, Invarsdóttir A, Jónasdóttir SH, Lindique P, Pollard RT, Rasmussen J, Richards K, Richardson K, Smerdon G, Speirs D (2004) Comparative ecology of overwintering *Calanus finmarchicus* in the northern North Atlantic, and implications for life-cycle patterns. *ICES J Mar Sci* 61:698–708
- Holliday DV, Pieper RE (1995) Bioacoustical oceanography at high frequencies. *ICES J Mar Sci* 52:279–296
- Irigoin X (2004) Some ideas about the role of lipids in the life cycle of *Calanus finmarchicus*. *Plankton Res* 26: 259–263
- Irigoin X, Titelman J, Harris RP, Harbour D, Castellani C (2003) Feeding of *Calanus finmarchicus* nauplii in the Irminger Sea. *Mar Ecol Prog Ser* 262:193–200
- Kaartvedt S (2000) Life history of *Calanus finmarchicus* in the Norwegian Sea in relation to planktivorous fish. *ICES J Mar Sci* 57:1819–1824

- Lavender K, Davis RE, Brechner Owens W (2000) Mid-depth recirculation observed in the interior Labrador and Irminger seas by direct velocity measurements. *Nature* 407:66–69
- MacLennan DN, Fernandes PG, Dalen J (2002) A consistent approach to definitions and symbols in fisheries acoustics. *ICES J Mar Sci* 59:365–369
- Magnusson J (1996) The deep scattering layers in the Irminger Sea. *J Fish Biol* 49:182–191
- McGehee DE, O'Driscoll RL, Traykovski LVM (1998) Effects of orientation on acoustic scattering from Antarctic krill at 120 kHz. *Deep-Sea Res II* 45:1273–1294
- Parsons TR, Lalli CM (1988) Comparative oceanic ecology of the plankton communities of the subarctic Atlantic and Pacific oceans. *Oceanogr Mar Biol* 26:317–359
- Pollard RT, Hay SJ, Williamson P, Moncoiffe G (2002) Biophysical studies of zooplankton dynamics in the northern North Atlantic: Winter (1st November–18th December 2001) Marine Productivity Cruise Report. NERC, Swindon, pp 112
- Sameoto D (1989) Feeding ecology of the Lantern Fish *Benthoosema glaciale* in a subarctic region. *Polar Biol* 9:169–178
- Sanders R, Brown L, Henson S, Lucas M (2004) New production in the Irminger Basin during 2002. *J Mar Syst* (in press)-doi:10.1016/j.jmarsys.2004.09.002
- Sigurðsson T, Rätz H-J, Pedchenko A, Mamylov V, Mortensen J, Bethke E, Stransky C, Björnsson H, Melnikov S, Bakay Y, Drevetnyak K (1999) Report of the joint Icelandic/German/Russian trawl-acoustic survey on pelagic redfish in the Irminger Sea and adjacent waters in June/July 1999. Annex to the North-Western Working Group Report 1999, International Council for the Exploration of the Sea, Copenhagen
- Sigurðsson T, Jónsson G, Pálsson J (2002) Deep scattering layer over the Reykjanes Ridge and in the Irminger Sea. Conference Manuscript CM 2002/M:09, International Council for the Exploration of the Sea, Copenhagen
- Tande KS, Miller CB (2000) Population dynamics of *Calanus* in the North Atlantic: results from the Trans-Atlantic Study of *Calanus finmarchicus*. *ICES J Mar Sci* 57:1527
- Watkins JL, Brierley AS (1996) A post-processing technique to remove background noise from echo integration data. *ICES J Mar Sci* 53:339–344